

## A New Current Control Algorithm for Torque Ripple Reduction of BLDC Motors

Tae-Sung Kim, Sung-Chan Ahn, Dong-Seok Hyun

Dept. of Electrical Engineering, Hanyang University, 17  
Haengdang-dong, Seongdong-ku, Seoul, 133-791 Korea

[redtea@ihanyang.ac.kr](mailto:redtea@ihanyang.ac.kr)

**Abstract** - The BLDC (Brushless DC) Motor is characterized by linear torque to current and speed to voltage. It has low acoustic noise and fast dynamic response. Moreover, it has high power density with high proportion of torque to inertia in spite of small size drive. However, when armature current is commutated, the current ripple is generated by the motor inductance components in stator windings and back-EMF. This current ripple caused to torque ripple. Therefore, it is difficult to apply the BLDC motor to a precision servo drive system.

In this paper, a new current control algorithm using fourier series coefficients is proposed. This proposed algorithm can minimize torque ripple due to the phase current commutation of BLDC motor. Simulation and Experimental results prove the effectiveness at the proposed algorithm through comparison with the conventional unipolar PWM method.

### I. INTRODUCTION

The BLDCM is the most suitable motor in application field with requiring fast dynamic response of speed, because it has high efficiency and can be easily controlled in a wide speed range. BLDCM has trapezoidal back-EMF waveform. Theoretically, when it is fed with rectangular phase current of 120° conduction, it produces constant torque without ripple. Generally, VSI (voltage source inverter) is used for achieving the rectangular current waveform rather than CSI (current source inverter), because the CSI is necessary to large inductor and only devices with reverse blocking capability can be used in spite of minimizing current ripple. But the current ripple is produced by the phase current commutation when VSI is used [1],[2].

Recently, a number of current controls have been proposed in order to reduce current ripple [3]-[7]. The typical methods are hysteretic current control and PWM current control. First of all, the former has high current control capability, but it is difficult to apply to device, which decreasing switching capacity because of switching frequency change in accordance with hysteretic bandwidth, back-EMF magnitude. In contrast, the latter has lower current control capability than the former. But it has the advantage of constant switching frequency of switching device.

PWM current control is divided into unipolar PWM method and bipolar PWM method. The general driving

method, unipolar PWM of 120° conduction makes fewer switching loss and current ripple, but lower dynamic response of current. As a result, it cannot be applied to application field like as servomotor demanding precision position control. On the contrary, bipolar PWM method makes higher dynamic response of current, but this method more switching loss and current ripple than unipolar PWM method. However, development of power electronic semiconductor device and current control method supplement fault of bipolar PWM.

In this paper, we proposed a new current control algorithm for reducing current ripple, which causes torque ripple mostly when BLDCM is operated. This algorithm using fourier series coefficients is not only simple but also operates optimal performance. Several simulation and experiment results proved effectiveness of proposed method.

### II. OPERATION OF THE BLDCM

#### 1) Modeling of BLDCM

The BLDCM drive block diagram is shown in Fig. 1.

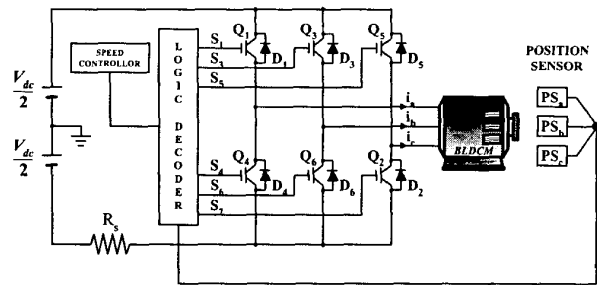


Fig. 1. Block diagram of BLDCM drive.

Assuming that self and mutual inductances are constant, the voltage equation of three phases is given by

$$\begin{pmatrix} V_{ap} \\ V_{bp} \\ V_{cp} \end{pmatrix} = \begin{pmatrix} R_s & 0 & 0 \\ 0 & R_s & 0 \\ 0 & 0 & R_s \end{pmatrix} \begin{pmatrix} i_a \\ i_b \\ i_c \end{pmatrix} + \begin{pmatrix} L_s & 0 & 0 \\ 0 & L_s & 0 \\ 0 & 0 & L_s \end{pmatrix} \frac{d}{dt} \begin{pmatrix} i_a \\ i_b \\ i_c \end{pmatrix} + \begin{pmatrix} e_a \\ e_b \\ e_c \end{pmatrix} \quad (1)$$

The torque equation is given by

$$T_e = \frac{e_a \cdot i_a + e_b \cdot i_b + e_c \cdot i_c}{\omega_m} \quad (2)$$

where,  $V_{ap}, V_{bp}, V_{cp}$ : Phase Voltage  
 $i_a, i_b, i_c$ : Phase Current  
 $e_a, e_b, e_c$ : Phase Back - EMF  
 $R_s$ : Phase Resistance  
 $L_s$ : Phase Inductance  
 $\omega_m$ : Angular Velocity

As Fig. 2 is shown, when phase currents of rectangular shape is input at the flat part of back-EMF waveform. It is shown that torque ripple is minimized through Eq (2). But the ideal currents input such as Fig. 2 is impossible actually due to inductance component in stator windings and back-EMF.

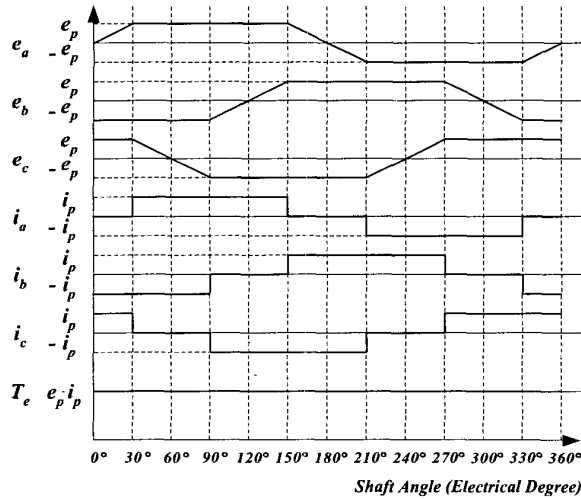


Fig. 2. Waveforms of back EMF and phase current of BLDCM.

As previously mentioned, to minimize torque ripple of the BLDCM, the unipolar PWM method, which makes the rectangular current of 120° conduction, are widely used as shown in Fig. 3.

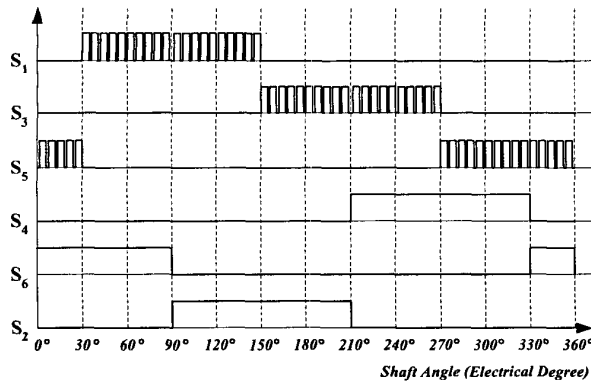


Fig. 3. Switching signals of unipolar PWM method.

However, unipolar PWM method has lower dynamic response of current control and is difficult to reduce torque ripple by current commutation. Accordingly, in this paper, a new current control algorithm is proposed. Applying SVPWM method to unipolar PWM method makes the PWM switching signal with a proposed current control algorithm. Consequently, the waveform of the PWM switching signal is similar to bipolar PWM as shown in Fig. 4

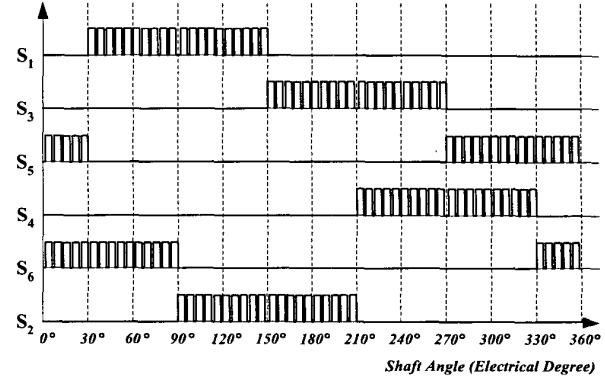


Fig. 4. Switching signals of bipolar PWM method.

## 2) Proposed current control algorithm

Now, if the phase current is assumed as rectangular shape, then its fourier series is followed.

$$i(t) = a_0 + \sum_{n=1}^{\infty} (a_n \cdot \cos n\omega t + b_n \cdot \sin n\omega t) \quad (3)$$

Since  $i(t)$  is an odd function,  $a_0$  and  $a_n$  is zero. Consequently, Eq. (3) can be written Eq. (4)

$$i(t) = \sum_{n=1}^{\infty} (b_n \sin n\omega t) \quad (4)$$

$$\text{Where, } b_n = \frac{4}{n\pi} \cos\left(\frac{n\beta}{2}\right)$$

$$n = 1, 3, 5, \dots$$

$$\beta = \pi/3 : \text{ commutation duration.}$$

From Eq. (4), harmonics of 3 multiples are eliminated because the motor is wound Y winding. Rectangular phase current of 120° conduction is made by summation of each harmonic sinewaveform. After reference speed of direct value divided into each harmonic coefficient. As shown in Fig. 5, we can find the waveforms, which made by adding these coefficients, are similar to the command.

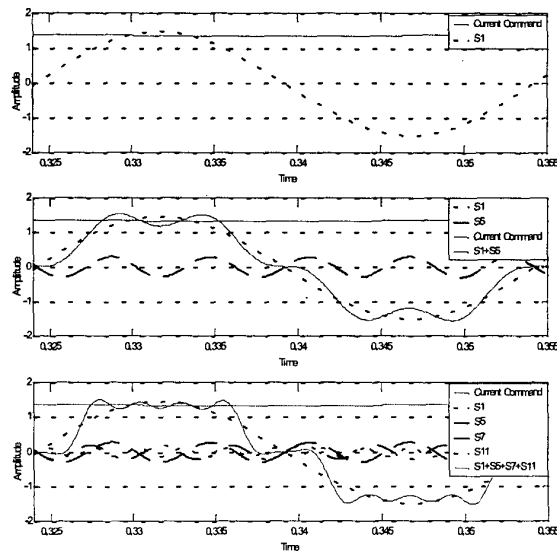


Fig. 5. Current command value and summation of each harmonic.

The Fig. 6 shows, firstly, current command ( $i_q^*$ ), contains all harmonic components, is obtained by PI speed controller. Secondly, This current command ( $i_q^*$ ) is separated into each harmonic component ( $i_{q1}^*$ ,  $i_{q5}^*$ ,  $i_{q7}^*$ , and other harmonics) by using the Eq. (4), current command ( $i_q^*$ ) is divided by  $b_n$  each other and then transformed into stationary frame components ( $i_{\alpha 1}^*$ ,  $i_{\beta 1}^*$ ,  $i_{\alpha 5}^*$ ,  $i_{\beta 5}^*$ , ...). Each harmonic component in stationary frame is added each frame, respectively. This summation value is current command ( $i_{\alpha}^*$ ,  $i_{\beta}^*$ ). In the last, three phase currents fed to current controller are transformed to stationary frame and PI current control can be controlled  $i_{\alpha}$  and  $i_{\beta}$ , respectively.

After these processing, the neutral voltage will be compensated with feedforward compensation because the inverter neutral voltage and the motor neutral voltage are different. In this paper, phase current will be more rectangular than other method because typical rectangular shape will be analyzed by fourier series, then BLDCM is controlled with minimized torque ripple than typical methods.

### III. SIMULATION RESULTS

In order to verify the proposed control algorithm simulation was performed by using ACSL. Table I shows the simulation condition. Figs. 7 and 8 show simulated input phase currents and torque waveforms of conventional method and proposed one. Figs. 9 and 10 show simulated reference speed, actual speed, torque, and phase current waveforms of conventional method and proposed one.

As shown Fig. 7(a), when input phase current is commutated, current ripple is generated seriously. Consequently, torque ripple is also generated. However, if current control is performed with proposed algorithm, as shown Fig. 8, ideal rectangular current of 120° conduction is obtained. Therefore, torque ripple is reduced remarkably. Additionally, as compared with Figs. 7 and 8 the greater part of torque ripple in Fig. 7 is due to the commutation of the current in BLDCM. On the other hand, most part of torque ripple in Fig. 8 is due to the switching ripple, which is occurred by using inverter. Fig. 9 shows the start up waveforms using conventional method and Fig. 10 shows the startup waveforms using proposed method when the speed reference is abruptly changed from 0 to 1200 rpm. It takes 0.32 seconds to steady state in Fig 9(b). On the other hand, It takes 0.12 seconds to steady state in Fig 10(b). Comparing Fig 9(b) with Fig 10(b) illustrates conspicuously improved speed response characteristics in transient state. When BLDCM is operated using proposed algorithm, more rectangular phase current is obtained despite of the switching ripple, and then torque ripple is minimized.

### IV. EXPERIMENTAL RESULTS

The BLDCM inverter stack using in experiment is implemented with IPM (Intelligent Power Module) devices. TMS320C31 DSP (Digital Signal Processor) controller is used as the main controller and control algorithm is expected with sampling time of 150  $\mu$ s. Look-up table is used for harmonic calculation. Figs. 11 and 12 are obtained in condition of 1200 rpm and 1 Nm when input current is in steady state. Figs. 11 and 12 show experimented input phase currents and torque waveforms of conventional method and the proposed one. Figs. 13 and 14 show experimented reference speed, actual speed, torque, and phase current waveforms of conventional method and proposed one. Experimental results agree with simulation results.

Table I  
Parameters of BLDCM

Rated Voltage	V	310 [V]
Rated Torque	$T_e$	2 [Nm]
Resistance	$R_s$	7.3 [ $\Omega$ ]
Inductance	$L_s$	20.3 [mH]
Back EMF Constant	$K_e$	0.3 [V/(rad/sec)]
Poles	P	4

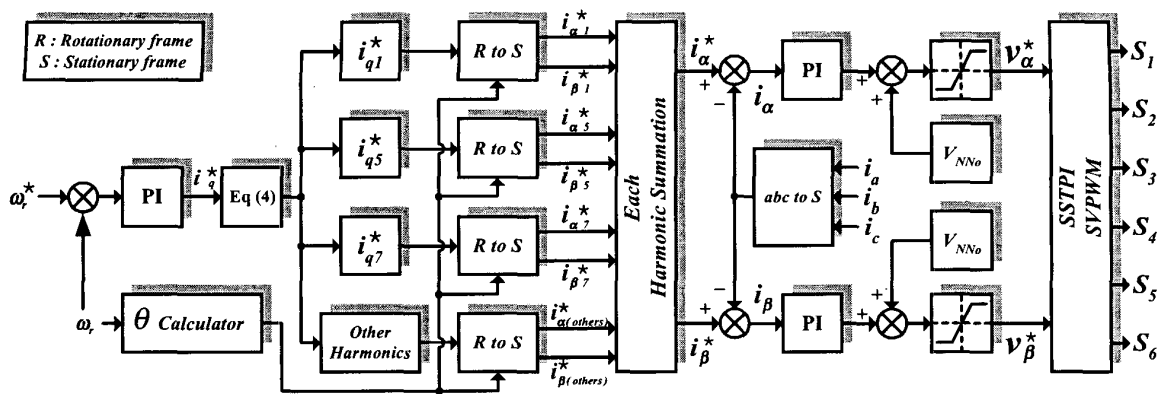


Fig. 6. Block diagram of proposed current control algorithm.

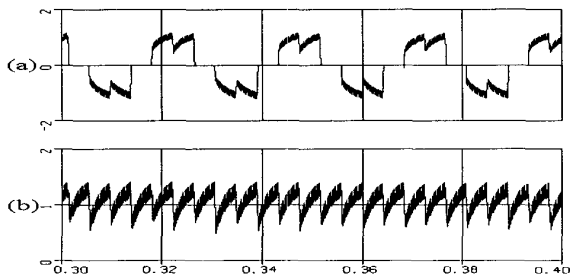


Fig. 7. Detail Input phase current and torque waveforms  
At load 1 [Nm] using conventional method in simulation  
(a) Phase current [A]      (b) Torque [Nm]

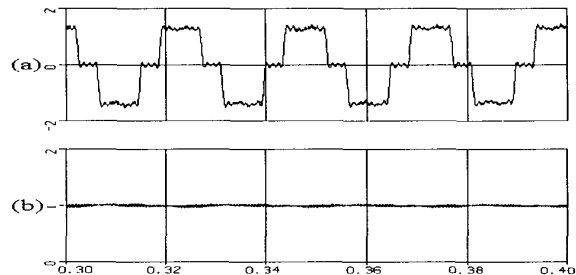
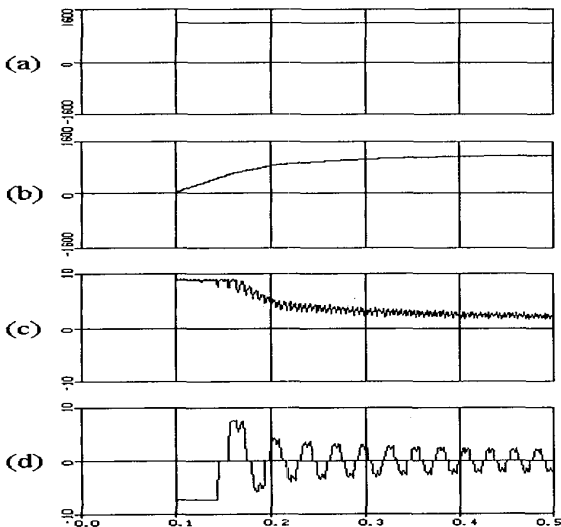
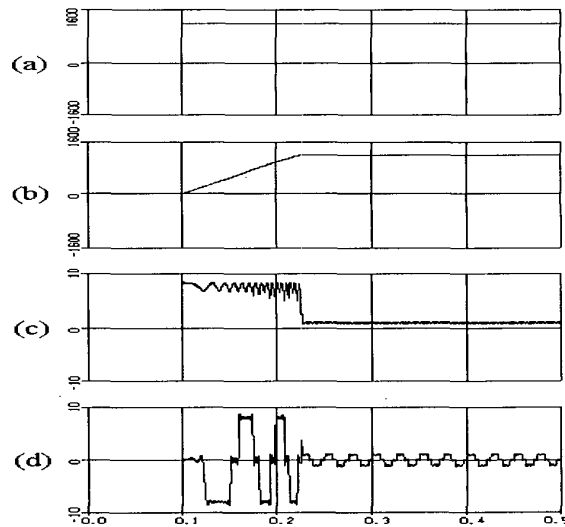


Fig. 8. Detail Input phase current and torque waveforms  
At load 1[Nm] using proposed method in simulation  
(a) Phase current [A]      (b) Torque [Nm]



**Fig. 9. Startup waveforms using conventional method in simulation**

(a) Reference speed[rpm]      (b) Actual speed[rpm]  
(c) Torque[Nm]                  (d) Phase current[A]



**Fig. 10. Startup waveforms using proposed method in simulation**

(a) Reference speed[rpm]      (b) Actual speed[rpm]  
(c) Torque[Nm]                  (d) Phase current[A]

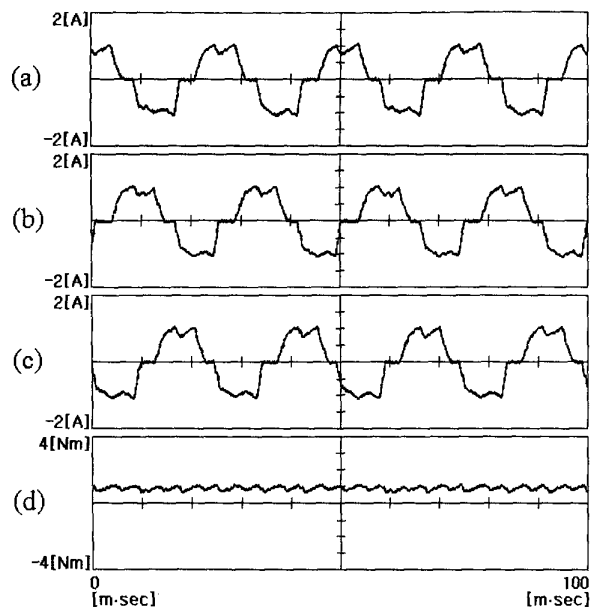


Fig. 11. Input phase currents and torque waveforms at load 1[Nm] using conventional method in experimental result.

(a) a phase current [A] (b) b phase current [A]  
(c) c phase current [A] (d) Torque [Nm]

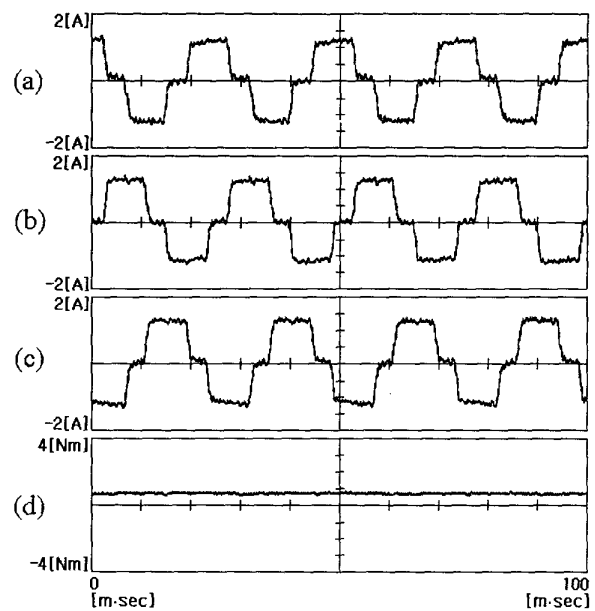


Fig. 12. Input phase currents and torque waveforms at load 1[Nm] using proposed method in experimental result

(a) a phase current [A] (b) b phase current [A]  
(c) c phase current [A] (d) Torque [Nm]

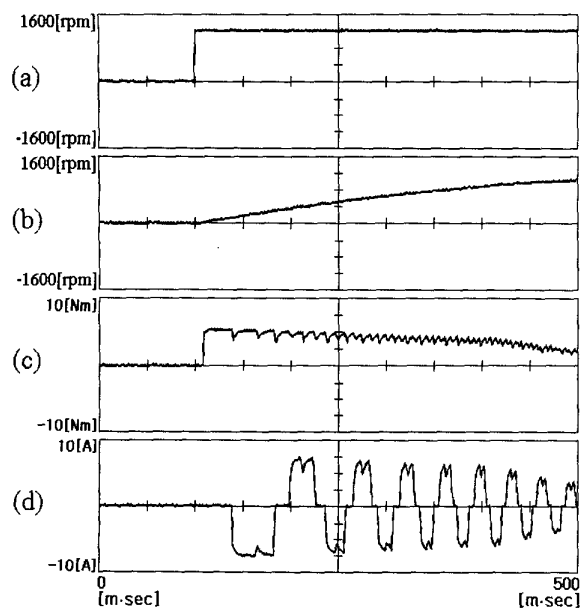


Fig. 13. Startup waveforms using conventional method in experimental result.

(a) Reference speed [rpm] (b) Actual speed [rpm]  
(c) Torque [Nm] (d) Phase current [A]

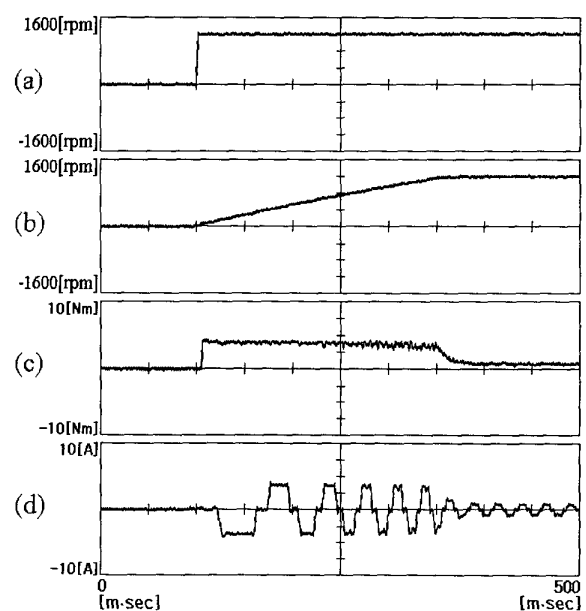


Fig. 14. Startup waveforms using proposed method in experimental result.

(a) Reference speed [rpm] (b) Actual speed [rpm]  
(c) Torque [Nm] (d) Phase current [A]

## V. CONCLUSION

In this paper, a new algorithm was proposed to reduce torque ripple, which is generated by unipolar PWM method in conventional BLDCM drive. At proposed algorithm, the current harmonic is calculated within a permitted degree using fourier series coefficients. After transforming these harmonic components into stationary frame, phase current similar to rectangular waveform is generated by applying SVPWM methods to voltage command which is caused by current control. It reduces current ripple so that noise vibration, which is produced by driving BLDCM, is significantly removed. Moreover, using the look-up table for harmonic calculation caused to shorten the calculation time without a highly efficient CPU.

If the proposed algorithm is applied to home appliances requiring low noise such as a room ventilator of air conditioner, compressor of a refrigerator, office automation, audio, computer device and so on, it is expected with improvement in quality.

## VI. REFERENCE

- [1] T. J. E. Miller, *Brushless Permanent-Magnet and Reluctance Motor Drives*, Clarendon Press, Oxford 1989.
- [2] P. Pillay and R. Krishnan, "Modeling, Simulation, and Analysis of Permanent - Magnet Motor Drives, Part I : The Permanent - Magnet Synchronous Motor Drive," *IEEE Trans. Industrial. Applicat.*, vol. 25, no. 2, Mar/Apr. 1989, pp. 265-273.
- [3] R. Carlson, M. Lajoie-Mazenc, and J. Fagundes, "Analysis of Torque Ripple Due to Phase Commutation in Brushless dc Machines," *IEEE Trans. Industrial. Applicat.*, vol. 28, no. 3, May/June. 1992, pp. 632-638.
- [4] C. S. Berendsen, G. Champenois, and A. Bolopion, "Commutation Strategies for Brushless DC Motors : Influence on Instant Torque," *IEEE Trans. Power Electronics*, vol. 8, no. 2, Apr. 1993, pp. 231-236.
- [5] T. M. Jahns and W. L. Soong, "Pulsating Torque Minimization Techniques for Permanent Magnet AC Motor Drives - A Review," *IEEE Trans. Industrial. Electronics*, vol. 43, no. 2, Apr. 1996, pp. 321-330.
- [6] S. K. Safi and P. P. Acarnley and A. G. Jack, "Analysis and simulation of the high-speed torque performance of brushless DC motor drives," *IEE. Proc. Electronics. Power Appl.*, vol. 142, no. 3, May. 1995, pp. 191-200.
- [7] D. C. Hanselman, "Minimum Torque Ripple, Maximum Efficiency Excitation of Brushless Permanent Magnet Motors," *IEEE Trans. Industrial. Electronics*, vol. 41, no. 3, June. 1994, pp. 292-300.